ISLAMIC UNIVERSITY OF TECHNOLOGY (IUT)

PERFORMANCE ANALYSIS OF OPTIMIZED VORTEX TUBE GENERATED AIR AS COOLANT IN MACHINING PROCESS BY CFD AND FEA METHOD

B.Sc. Engineering (Mechanical) THESIS

BY

A A MUBASSHIR (141455)
ANWAR SHAFE (141426)

SUPERVISED BY

PROFESSOR DR. MD. ANAYET ULLAH PATWARY

NOVEMBER 2018

PERFORMANCE ANALYSIS OF OPTIMIZED VORTEX TUBE GENERATED AIR AS COOLANT IN MACHINING PROCESS BY CFD AND FEA METHOD

BY

A A MUBASSHIR
STUDENT NO: 141455

ANWAR SHAFE
STUDENT NO: 141426

A THESIS PRESENTED TO THE DEPARTMENT OF MECHANICAL AND CHEMICAL ENGINEERING, ISLAMIC UNIVERSITY OF TECHNOLOGY DHAKA IN PARTIAL FULFILMENT OF THE REQUIREMENT FOR THE AWARD OF DEGREE FOR

BACHELOR OF SCIENCE (B. Sc.) IN MECHANICAL ENGINEERING.

NOVEMBER 2018

Candidate's Declaration

It is hereby declared that this thesis or any part of it has not been submitted elsewhere for the award of any degree or diploma.

Signature of the Candidate

_____

A A Mubasshir
Student No.: 141455
Session 2017-2018
Department of Mechanical and Chemical Engineering (MCE)
Islamic University of Technology (IUT), OIC
Board Bazar, Gazipur
Dhaka, Bangladesh.

_____

Anwar Shafe
Student No.: 141426
Session 2017-2018
Department of Mechanical and Chemical Engineering (MCE)
Islamic University of Technology (IUT), OIC
Board Bazar, Gazipur
Dhaka, Bangladesh.

Signature of the Supervisor

_____

Prof. Dr. Md. Anayet Ullah Patwary
Professor
Department of Mechanical & Chemical Engineering (MCE)
Head
Department of Research, Extension Advisory, Services & Publications (REASP)
Islamic University of Technology (IUT), OIC
Board Bazar, Gazipur
Dhaka, Bangladesh.

Certificate of Approval

The thesis titled "**PERFORMANCE ANALYSIS OF OPTIMIZED VORTEX TUBE GENERATED AIR AS COOLANT IN MACHINING PROCESS BY CFD AND FEA METHOD**" submitted by A A Mubasshir and Anwar Shafe bearing Student No. 141455 and 141426 respectively of Academic Year 2017-2018 has been found as satisfactory and accepted as partial fulfillment of the requirement for the degree of Bachelor of Science in Mechanical Engineering on 13 November, 2018.

Dr. Md. Anayet Ullah Patwari
Professor
Department of Mechanical and Chemical Engineering
Islamic University of Technology (IUT)
Board Bazar, Gazipur
Dhaka, Bangladesh.

Dr. Zahid Hoosain
Professor and Head
Department of Mechanical and Chemical Engineering
Islamic University of Technology (IUT)
Board Bazar, Gazipur
Dhaka, Bangladesh.

Acknowledgements

We would like to begin by saying Alhamdullilah and grateful to Almighty Allah who made it possible for us to finish this project successfully on time. Equally say a big thank to my supervisor Dr. Md. Anayet Ullah Patwary, Professor, Department of Mechanical and Chemical Engineering, IUT for all his support, ideas about experiments, discussions, time and for explaining so patiently the hard topics and checking this thesis and papers above all his care and concern. These will ever remain in our memory. Thanks to our examiners for their constructive ideas, suggestions and double checking our work. Special thanks to all faculties for their support and encouragement throughout the period of our studies.

We would like to say a big thank you to the Head of Department Professor Dr. Zahid Hossain for his continues encouragement and support during the period of our studies. Finally, we will like to express our lasting gratitude to our family members for their patience, support, encouragement, enthusiasm and prayers.

Table of Contents

List of Figures

List of Tables

Abstract

Coolants are used to negate or minimize the thermal stresses developed during any machining process. However, some environmental and health issues are associated with traditional coolant. Documented health issues include Cancer, Dermatitis, Respiratory irritation, Asthma and Hypersensitivity Pneumonitis. In this experimental study, the effect of Ranque-Hilsch vortex-tube generated cold air/hot air is observed in a machining process as a replacement for traditional liquid coolant. The optimum dimension for maximum energy separation is obtained by trial method using computational fluid dynamics (CFD). For available compressed air of 6-8 bar, the optimum dimensions and geometry of the vortex-tube are: length (L) 300 mm, tube diameter (D) 20mm, cold outlet diameter (d_c) 6mm, inlet nozzle diameter (d_{in}) 5mm, angle of control valve (φ) 50 degree. Temperatures in the hot outlet and cold outlet are T_{hot}= 33℃ and T_{cold} = 14℃ are observed in the CFD model. Optimized vortex-tube outputs are then used as input parameters in AdvantEdge 3D software for studying post-machining characteristics of the workpiece. The chief parameters representing the machining quality are stress developed in the tool and workpiece and chip thickness. Machining quality with vortex-tube supplied air, conventional coolant and no coolant are then compared.

Chapter 1 Introduction

The counterflow vortex tube is a tubular thermal device without any moving parts which separates a compressed flow of fluid into two layers with lower pressures. One of the layers is of high temperature and the other is of low temperature. This phenomenon of energy separation was first observed by Ranque [1]. Later, Hilsch [2] studied these effects in detail. Since then a number of intensive experimental and analytical studies of Ranque-Hilsch effect have been carried out. According to these studies when compressed gas is injected through one or more tangential nozzles into the vortex tube a strong circular flow field is established. The high-pressure gas expands through the tube and achieves a high angular velocity causing a vortex-type flow in the tube. This vortex in the inlet region causes pressure distribution of the flow in the radial direction. This phenomenon results in a free vortex which causes the peripheral warm stream and a forced vortex which causes the central cold stream [3]. The vortex tube consists of a circular tube, one or more tangential nozzles for supplying compressed fluid and a control valve. By adjusting the control valve at the hot exit it is possible to vary the fraction of the incoming gas that leaves through the cold exit. The schematic of a counterflow vortex tube is shown in Fig-1.

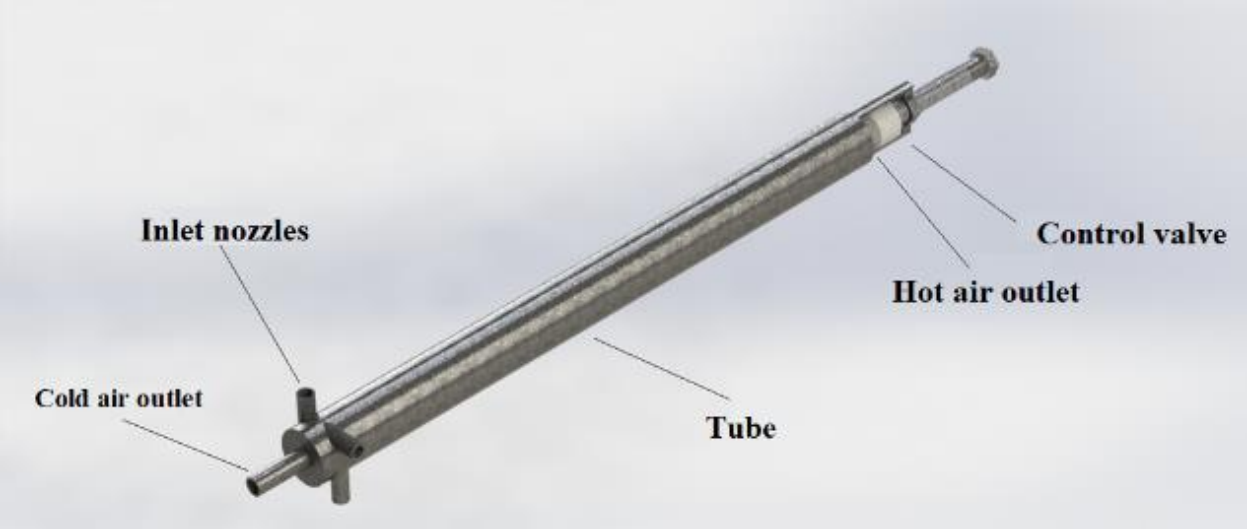

Figure 1: Counter Flow Vortex Tube

In this paper, we will simulate the effects of using vortex tube generated cold air as a replacement for traditional coolants. Traditional coolants can be of several types including Straight Oils, Soluble Oils, Synthetic and Semi-Synthetic. Some health and hazard issues are associated with traditional coolants. To name a few, Straight Oils have poor heat dissipating capabilities and risk of fire in high-temperature applications; Soluble Oils are susceptible to bacterial growth and cleaning the workpiece is harder; Synthetic coolants are easily contaminated by other fluids and also forms residues. Semi-Synthetics are the better option against above-mentioned ones, but it also has health issue involving Dermatitis. For this reason, we studied the cold air from the tube as a replacement for traditional liquid coolants, because it doesn't pollute the environment and less hazardous for machine operators. Another advantage of the vortex tube is that it includes no moving parts.

The purpose of this study is to compare the performance of traditional coolants, vortex generated air and without any coolants during a short turning operation. The performance parameters include stress developed in the workpiece, the average material removal rate (MRR), Surface Roughness (R_A), and average cost per volume of material removed per second.

The point of choosing turning operation for this study is it's the most common of all material removal process. The turning process involves a rotating workpiece and a linearly moving single point cutting tool. The workpiece is held by a rotating jaw called Chuck. The tool is mounted on the tool post which traverses linearly according to predetermined speed measured in unit of distance traveled per unit time. The traverse rate is called feed. Single point cutting tools can be of various types. Each type is intended for specific type of turning.

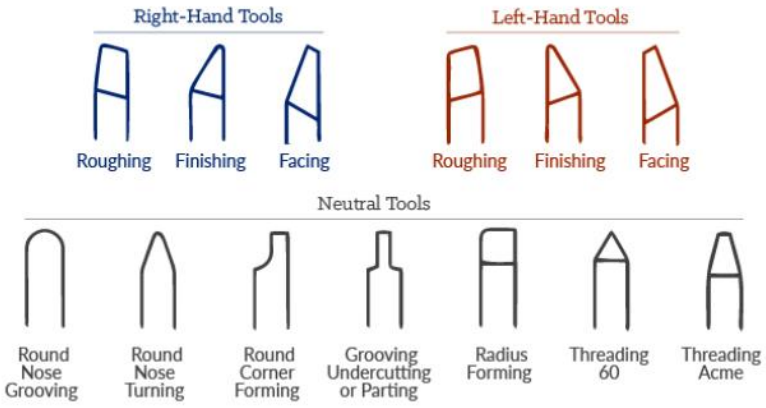

Figure 2: Cutting tools.

A limitation of the turning process is that it can only be done to produce cylindrical round shapes. Typically a lathe is used for turning. It can be manually operated or automatically operated. The downside of manual turning is that it needs to be supervised continually, whereas automated turning doesn't.

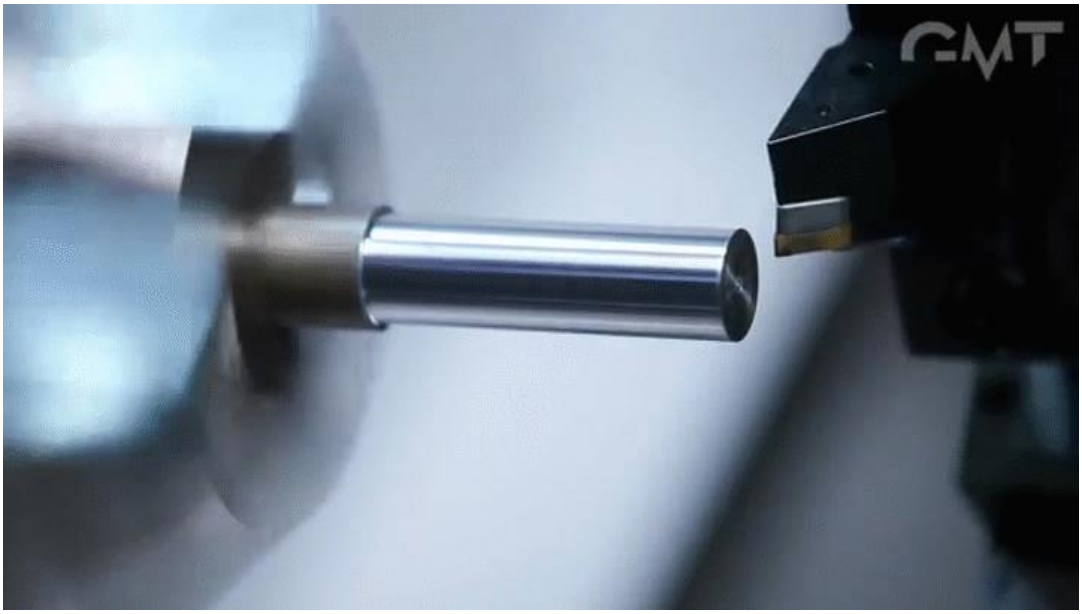

Figure 4: Turning Operation

This paper is arranged and divided into parts. First, we performed the CFD modeling of the vortex tube under available conditions. In this study, the comparative analysis of the vortex tube for various parameters has been carried out. From this study, optimum geometry and corresponding air temperatures at the outlets have been obtained. This data is then used as conditions under which the machining operation is taking place. The software used for simulating the operation is Third Wave Systems' AdvantEdge 3D (v 11.7). Hot air is used for heating the workpiece and cold air is used as a coolant so that the hot and cold outlet temperatures are used later as initial workpiece temperature and coolant temperature respectively. The same tool and workpiece geometry are applied in two different cases. One is with traditional coolant and the other is without any coolant. Next, the results are obtained and an Apple to Apple comparison is done involving all three cases. Finally, the abovementioned comparison parameters are studied.

Chapter 2 Literature Review

Vortex Tube:

The vortex tube, also known as the Ranque-Hilsch vortex tube, is a mechanical device that separates a compressed gas into hot and cold streams. The gas emerging from the "hot" end can reach temperatures of 200^0C (392^0F), and the gas emerging from the "cold end" can reach −50 °C (−58 °F). It has no moving parts. Pressurized gas is injected tangentially into a swirl chamber and accelerated to a high rate of rotation. Due to the conical nozzle at the end of the tube, only the outer shell of the compressed gas is allowed to escape at that end. The remainder of the gas is forced to return in an inner vortex of reduced diameter within the outer vortex.

In 1931, G. Ranque , a French engineer, stumbled upon a new method or separating a gas stream into regions or high and low total temperatures in a vortex flow; this led to the discovery of the so-called vortex tube. The work of Ranque lay undeveloped until Rudolph Hilsch became interested in the vortex tube in relation to his low temperature experiments and published his findings in the mid-forties. Since then, the Ranque-Hilsch tube or vortex tube has been the subject of numerous investigations. These investigations have been involved not only with the Ranque-Hilsch vortex cooling effect per se, but also with the applications of vortex tubes to other purposes such as the containment of gases, with different densities, within the vortex field. In the Ranque-Hilsch tube or vortex tube, compressed air enters the vortex chamber first, where it is set into a swirling motion by passing through a swirl generator, a stationary ring with tangentially drilled slots. Once within the tube, the swirling air separates by itself into two streams of different total temperatures: the hotter air near the tube periphery and the colder one at the centerline. In the conventional counterflow Ranque-Hilsch tube the cold air is extracted from an orifice located near the inlet and the hot air escapes from the other end, where a flow controlling valve is located. The counterflow movement of the air is caused by the difference between the lowered axial pressure at the center and the atmospheric pressure. By adjusting the valve, the temperature and the relative flow rate of the cold and hot streams can be varied. Even by closing the cold end orifice, however, the air flowing only in one direction can still produce the radial separation of the total temperature; this is called uniflow type. Because of its simpler flow pattern, it is convenient to adopt this uniflow

type for analysis and experiment throughout the present investigation. The extreme simplicity of the vortex tube which has no moving parts and the spectacular separation of hot and cold streams suggested that it can be used as an air-operated refrigerator without a motor. As long as the adequate air supply is available, temperature below zero degree can easily be obtained; the tubes are now commercially available and widely used in cooling applications. In spite of its implicity of design and its spectacular effect of producing hot and cold air simultaneously, the mechanism of total temperature separation has remained a subject of controversy. In fact, it has never been fully explained. Consequently, there is a need for fundamental study of the phenomenon with the efforts to clarify the Ranque-Hilsch effect. From a practical point, there exists an increasing demand for better understanding of the temperature separation and the Ranque-Hilsch effect. For example, the Ranque-Hilsch effect may be exploited for turbine cooling in aircraft engines; this opens up a possibility of reducing the specific fuel consumption. Therefore, the understanding of this effect is important. In the next chapters, a summary of the past hypotheses of the many theoretical and experimental studies will be described, followed by the discussion on a radically new mechanism based upon the phenomenon of acoustic streaming. This terminology will be defined later. The objective of present study is directed toward confirmation of the above theory by crucial experiments.

Although the radial gradient of static temperature exists in the swirling flow of the Ranque-Hilsch tube, the temperature separation at issue is that of total temperature and not of the static one. Hence, the effect can, by no means, be explained away as due to an isentropic expansion or compression caused by the radial pressure gradient in a vortex. Nor is it due to the Joule-Thomson effect, for the temperature separation observed in the tube is by far the larger.. Nor does the tangential velocity need to exceed the sonic velocity, despite some earlier belief to the contrary. The process defies an immediate explanation, to the extent that some even attributed this, in a lighter vein, to Maxwell's demon coming to life. As pointed out by Liepmann and Roshko [4], one cannot, in fact, explain this within the framework of steady flow and has to resort to some form of unsteadiness. This is because the material derivative of total temperature is given by in the absence of any appreciable heat conduction, viscous dissipation and external work. Were the process steady, the right hand side of the equation would obviously vanish, leading, contrary to what

actually happens, to the invariance of the total temperature along any streamline. Thus the flow must be unsteady. But the crucial issue to be resolved is this: what form of unsteadiness? Either random turbulence or some orderly disturbance? This is the heart of the matter that has remained unsettled. The oft-expressed turbulent - migration theories attribute the mechanism of the· Ranque-Hilsch effect to turbulent energy transfer in general and the random migration of flow in the radial direction in particular. Deissler and Perlmutter [5], Linderstrom-Lang [6]stated that the total temperature separation in the vortex tube depends on the contributions of turbulent shear work done by Reynolds stress corresponding to radial migration of tangential velocity and of turbulent heat transfer due to radial migration of thermal energy under pressure gradients (by expansion and contraction of eddies). The experimental evidences will now be discussed. Hartnett and Eckert [7], Keyes [8], Lay [9], Linderstrom-Lang, Reynolds [10], Savino and Ragsdale [11], Scheller and Brown [12], Takahama, Bruun and Sibulkin [13] have measured internal flows in the Ranque-Hilsch tube. In most of these reported studies, total temperatures, velocities or turbulence in the Ranque-Hilsch tube were taken at optimum cooling conditions. There, the forced vortex is always found at any swirl and it forms immediately near the tangential inlets. It occupies the entire cross section (except near the tube wall boundary layer) and remains so from the entrance to the exit. At this condition, no vestige of a free vortex is found even in the inlet. All the experimental data show that the separation of the total temperature between hot and cold streams is maximum right near the inlet. As air flows toward the exit, the degree of total temperature separation decreases in the axial direction due to dissipative effect. The turbulence level in the Ranque-IIilsch tube was measured by Sibulkin to be 3- 7%. The turbulent migration theories assert that turbulent energy transfer is necessarily involved with the temperature separation of the RanqueHilsch effect. If turbulence is the main catalytic agent, the theories fail to explain the following: why in the particular case of the Ranque-Hilsch tube turbulent migration can abruptly lead to a forced vortex and the sudden separation of total temperature (as observed by Hartnett and Eckert and others) while, in other swirling flow devices with the same tangential injection and turbulence level as for the case of Ranque-Hilsch tube, it can still retain a free vortex (plus forced vortex type in the center core) and virtually uniform total temperature in the radial direction. The other theories proposed by Sibulkin, Scheper appear to be open to equally serious objections. The experimental evidence on some aircraft engine test rig to be presented shortly seems to point toward a pure tone or periodic

disturbance as an agent of the Ranque-Hilsch effect. In the literature on the Ranque-Hilsch tube, the presence of intense periodic disturbances is widely observed. Hilsch, McGee, Savino and Ragsdale, Kendall, Ragsdale, and Syred and Beer [14] recounted, in one way or the other, the disturbances of pure tone type or the whistle. Sprenger even suggested that the mechanism of total temperature separation accomplished within the Ranque-Hilsch tube may be analogous to the one of the resonance tube, which is attributed to organized unsteadiness. In fact, Savino and Ragsdale recorded an incident where a loud screaming noise was accompanied by 10 - 20° F change in total temperature, but they did not give any explanation on its mechanism.

Chip Formation

The mechanism of chip formation is still not completely understood, although shear instability and crack initiation and growth are the two main theories supporting this phenomenon. According to A. Hosseini et al [15]. when machining of titanium and its alloys, the chip

is either formed by the propagation of crack from the exterior surface of the chip or development of adiabatic shear band which is primarily originated by the localized shear deformation. In case of adiabatic shear, the machining is dominated by thermal softening rather than strain hardening. Localization of Shear leads to significant periodic variation of machining forces and subsequently chatters vibration. Cyclic variation of machining forces is not a desirable phenomenon as it imposes fatigue to the cutting tool or may cause chipping or breakage of cutting tool. In order to achieve an acceptable metal removal rate (MRR) at reasonable cost, appropriate tools, machining conditions, and processing sequence in a specific way. To reduce the experimental cost, researcher always prefer a FEA model. Said it allows plastic and thermal process with considering numeric dependencies of physical constant as well as describe complicated geometries and kinematics. Many FEA is established to see the effect of rake, cutting speed, and feed. Some researcher have tried to establish their FEA model by validating their simulation result with experimental result There is also research to establish FEA model to predict tool wear.

The purpose of our study is to use the cold air generated from the cold outlet as coolant in the machining process of metals. A vortex-tube also produces a stream of hot air which will also be used as a heating fluid for the workpiece. As a heated metal has uniform microstructure it is believed to be helpful in machining. By studying the must be selected properly. Many researcher are taking the challenges to improve the machinability by improving tool life and reduce cost any previous works on this subject it is apparent that vortex tube generated coolant is not used as a coolant in machining. Before fabricating the vortex-tube it is necessary to find the optimal dimensions of the vortex-tube so that the temperature drop in the cold and hot outlet will be maximum. This is done with simulation software ANSYS. A trial and error approach was taken to find out the optimum dimensions for the vortex-tube. This is discussed in detail later on.

Chapter 3 CFD Modelling

3.1. Geometry

A three dimensional (3D) simulation of the vortex tube was carried out in this study. Due to the ease of simulation, an appropriate fluid body corresponding to the vortex tube in Fig-1 was used. The main component of the vortex tube is a 300mm long tube which was tested for four different diameters of 1.5mm, 2mm, 2.5mm, and 3mm. Once we got the best fit diameter for the vortex tube with only one input nozzle, we then observed the performance of the tube with different number of input nozzles. The numbers of input nozzles for which the performance of the tube was observed were 2, 4 and 6. All the input nozzles have the same diameter of 5mm. This vortex tube also consists of a cold-air outlet and a hot-air outlet. The cold-air outlet is aligned with the centerline of the tube and has a diameter of 6mm. Though the 3D model of the vortex tube possesses a control valve to regulate the amount of air coming out of the hot end, in this simulation a fixed area was used to reduce complexity. A cross-section view of the fluid body is shown in Fig-4.

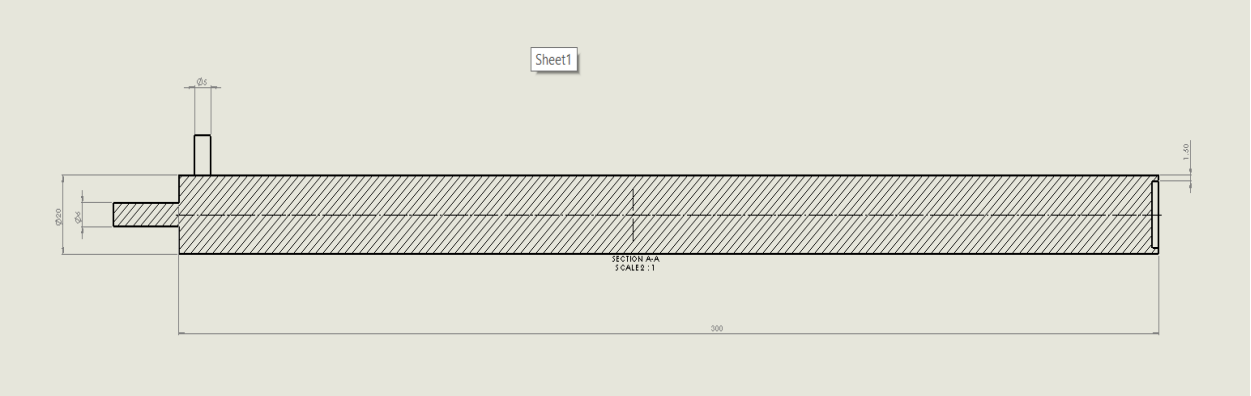

Figure 5: Cross Section of the Fluid Body

Table 1: Geometric details of vortex-tube

Parameters	Values
Tube length	300 mm
Tube diameters	15mm, 20mm, 25mm
Inlet nozzle diameter	5mm
Cold air outlet diameter	6mm
Hot air outlet diameter	6mm
Number of nozzles	2, 4, 6
Tube length	300 mm
Tube diameters	15mm, 20mm, 25mm
Inlet nozzle diameter	5mm
Cold air outlet diameter	6mm
Hot air outlet diameter	6mm
Number of nozzles	2, 4, 6

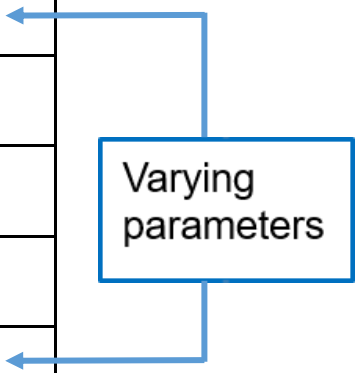

3.2. Meshing

A mesh consisting of 87800 grid elements was used in this study. The elements are concentrated in regions where large gradients in velocity and pressure are present. To achieve this, Refinement operation was performed in the inlet plane, hot exit and the core region of the vortex tube where energy separation occurs [16] . This vortex tube geometry under consideration has suitable values corresponding to mesh quality parameters. The table below shows that the mesh quality parameters have values that are well within the range of a good quality mesh. A good quality mesh raises the probability of accurate prediction for the numerical model.

Table 2: Average values of mesh quality parameters.

Parameters of mesh quality	Average Value	Recommended values
Skewness	0.31396	For perfect mesh skewness is 0 For the worst mesh skewness is 1 [17]
Orthogonal quality	0.83933	For perfect mesh orthogonal quality is 1 For the worst mesh orthogonal quality is 0 [18]
Warping factor	0.04957	For perfect mesh warping factor is 0 For the worst mesh warping factor is 1 [19]

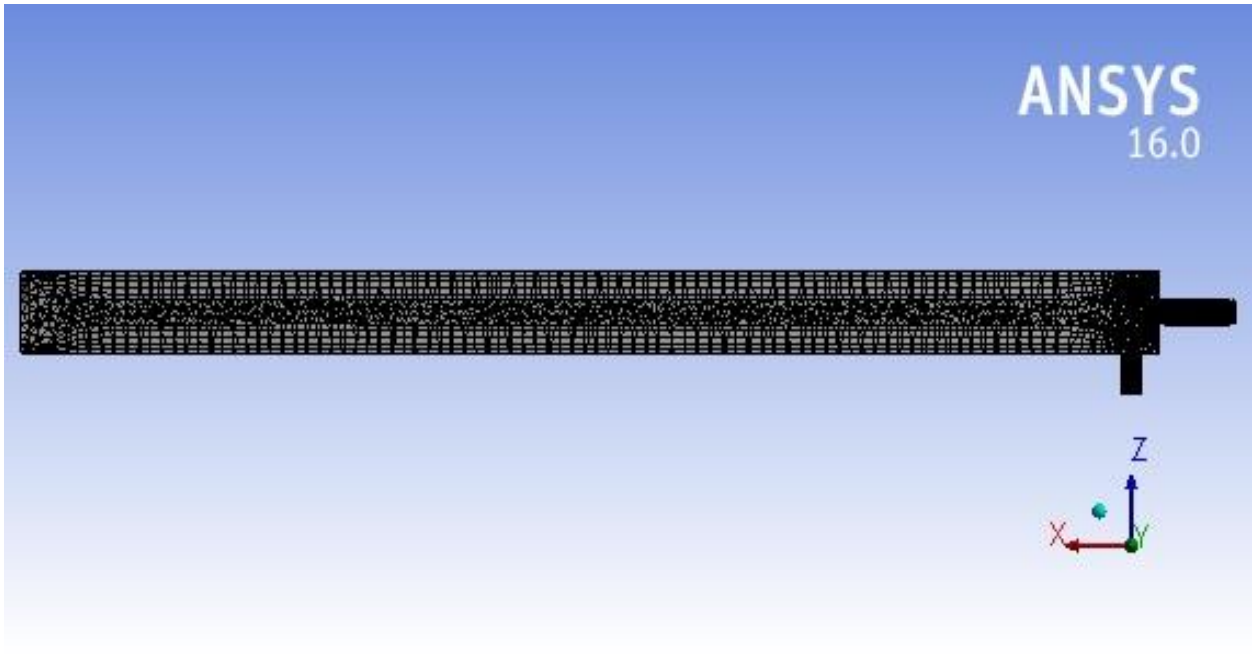

Figure 7: Refined mesh at the core region of the tube

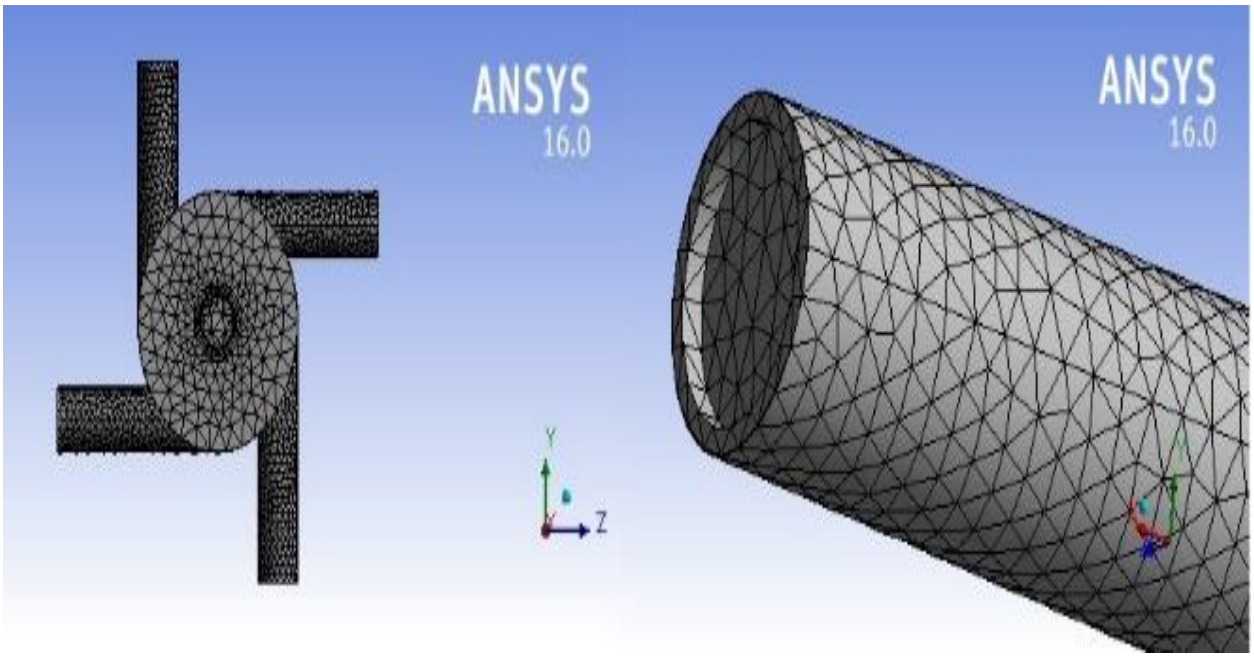

Figure 6: Refined mesh at the inlet and outlet region.

3.3. Numerical Modelling

This study of vortex tube involves swirling or rotating flow. In swirling flow, conservation of angular momentum results in the creation of a free vortex flow in which circumferential velocity w increases as the radius decreases and then decays to zero at r=0 due to the action of viscosity. For an ideal free vortex the circumferential forces are in equilibrium with radial pressure gradient.

$$\frac{\partial p}{\partial r} = \frac{\rho w^2}{r}$$

For non-ideal vortices the radial pressure gradient also changes affecting the radial and axial flows. The strength of the swirl is gauged by the swirl number S, defined as the ratio of the axial flux of angular momentum to the axial flux of the axial momentum.

$$S = \frac{\int r w \vec{v} \cdot d\vec{A}}{\bar{R} \int u \vec{v} \cdot d\vec{A}}$$

Where R is the hydraulic radius.

If any flow has a swirl number which is less than 0.5, then that flow can be referred to as weak or moderate swirl flow. Any flow with a swirl number greater than 0.5 can be referred to as highly swirling flow. The k-ε model shows better accuracy while predicting weak or moderate swirl flow. As we have weak or moderate swirl flow in the vortex tube, the Standard k- ε Model was selected as the numerical model.

The standard *k-ε* model is the first two-equation *k-ε* model published in the turbulence modeling literature and has been extensively applied and modified for its acceptable accuracy for computing wide range of industrial flows.

The k-ε model belongs to the class of two-equation models, in which model transport equations are solved for two turbulence quantities - i.e., k and ε in the k- ε model. From these two quantities can be formed a length scale ($L = k^{3/2}/\varepsilon$), a timescale (T= k/ε), a quantity of dimension υ_T (k^2/ε) etc. In addition to the turbulent viscosity hypothesis, the k-E model consists of

(i) The model transport equation for k (Eq. 1).

(ii) The model transport equation for ε (Eq. 2) and

(iii) The specification of the turbulent viscosity as

$$\nu_T = C_\mu k^2/\varepsilon,$$

Where Cμ=0.09 is one of five model constant.

This model is included in Fluent [8] as a standard *k-ε* model and employs the wall function for computational efficiency. The transport equation for turbulence kinetic energy *k* is an exact equation while the transport equation for turbulent dissipation (ε*)* is formulated using physical reasoning. The following are the transport equations for *k* and *ε* developed by Launder and Spalding [9]

$$\frac{\partial \rho k}{\partial t} + \frac{\partial \rho u_i k}{\partial x_i} = -\rho \overline{u_i u_j} \frac{\partial u_i}{\partial x_i} + \frac{\partial}{\partial x_i}\left[\rho\left(\nu_l + \frac{c_\mu k^2}{\sigma_k \epsilon}\right)\frac{\partial k}{\partial x_i}\right] - \rho\varepsilon$$

$$\frac{\partial \rho \varepsilon}{\partial t} + \frac{\partial \rho u_i \varepsilon}{\partial x_i} = -C_{\varepsilon 1}\rho \overline{u_i u_j} \frac{\partial u_i}{\partial x_i}\frac{\varepsilon}{k} + \frac{\partial}{\partial x_i}\left[\rho\left(\nu_l + \frac{c_\mu k^2}{\sigma_\varepsilon \epsilon}\right)\frac{\partial \varepsilon}{\partial x_i}\right] - C_{\varepsilon 2}\rho\frac{\varepsilon^2}{k}$$

$$\mu_t = \frac{\rho C_\mu k^2}{\varepsilon}$$

3.4. Boundary Condition

The CFD model is a two-dimensional model using axis-symmetry which was developed using Fluent 16.0. All the CFD simulations have been performed in steady state mode using pressure based implicit solver. Steady state assumption is justified because during experimental investigations, readings are always recorded after steady state values of temperatures and pressures at various locations are obtained. The flow inside the vortex tube is essentially compressible and subsonic. Hence, density of air has been modelled using ideal gas assumption.

The inlet of the vortex tube is assigned the boundary condition of pressure inlet for which the values of Total pressure, Supersonic pressure, Turbulent intensity, Turbulent viscosity ratio and Temperature are respectively 8atm, 7.93atm, 5%, 10 and 298 K. The hot and cold end are considered as pressure outlet which are open to atmosphere. Gravity was neglected and foe all the simulations, the energy equation has been activated.

To set the convergence criteria, default values of residuals of the order of 106 were used for energy while it was 103 for all other quantities. Wall of the vortex tube is assumed to be stationary and adiabatic with no-slip boundary condition. The properties of air considered for this simulation are Cp = 1006.43 J kg1 K1, k = 0.0242 W m1 K1, M = 28.966 kg kmol1, μ = 1.7894e-05.

3.5. Result Analysis

Selection of optimum geometry for the vortex tube was carried out in two steps. First, we selected the best fit diameter of the vortex tube by trial method on the basis of temperature difference. Then, we selected the best fit inlet nozzle number for selected tube diameter on the basis of velocity ratio.

Simulation on same geometric model which has one inlet but varies only on vortex-tube diameter was carried out. Temperature along the axis of rotation (z) was plotted. After the comparison of results, vortex tube with a diameter of 20mm was selected as this case showed the

highest temperature at hot-outlet and the lowest temperature at cold-outlet. This result shows **consistency** with the results of previous studies [20].

Table 3: Comparison of temperature along the rotational axis (Z axis)

Z	temperature for tube of d=15	temperature for tube of d=20	temperature for tube of d=25
2.69E-01	2.89E+02	2.33E+02	2.64E+02
2.59E-01	2.76E+02	2.40E+02	2.70E+02
2.48E-01	2.78E+02	2.47E+02	2.75E+02
2.38E-01	2.89E+02	2.53E+02	2.94E+02
2.28E-01	2.89E+02	2.65E+02	2.96E+02
2.17E-01	2.90E+02	2.72E+02	2.96E+02
2.07E-01	2.90E+02	2.80E+02	2.97E+02
1.97E-01	2.91E+02	2.88E+02	2.97E+02
1.86E-01	2.91E+02	2.93E+02	2.97E+02
1.76E-01	2.92E+02	2.95E+02	2.97E+02
1.55E-01	2.93E+02	2.95E+02	2.98E+02
1.34E-01	2.95E+02	2.95E+02	2.98E+02
1.24E-01	2.96E+02	2.95E+02	2.98E+02
1.14E-01	2.96E+02	2.92E+02	2.98E+02
1.03E-01	2.97E+02	2.89E+02	2.98E+02
8.28E-02	2.97E+02	2.75E+02	2.98E+02
7.24E-02	3.04E+02	2.69E+02	2.98E+02
6.21E-02	3.08E+02	2.64E+02	2.98E+02
5.17E-02	2.98E+02	2.61E+02	2.98E+02
4.14E-02	2.84E+02	2.74E+02	2.89E+02
3.10E-02	2.91E+02	3.12E+02	3.06E+02
1.03E-02	3.15E+02	3.48E+02	3.29E+02

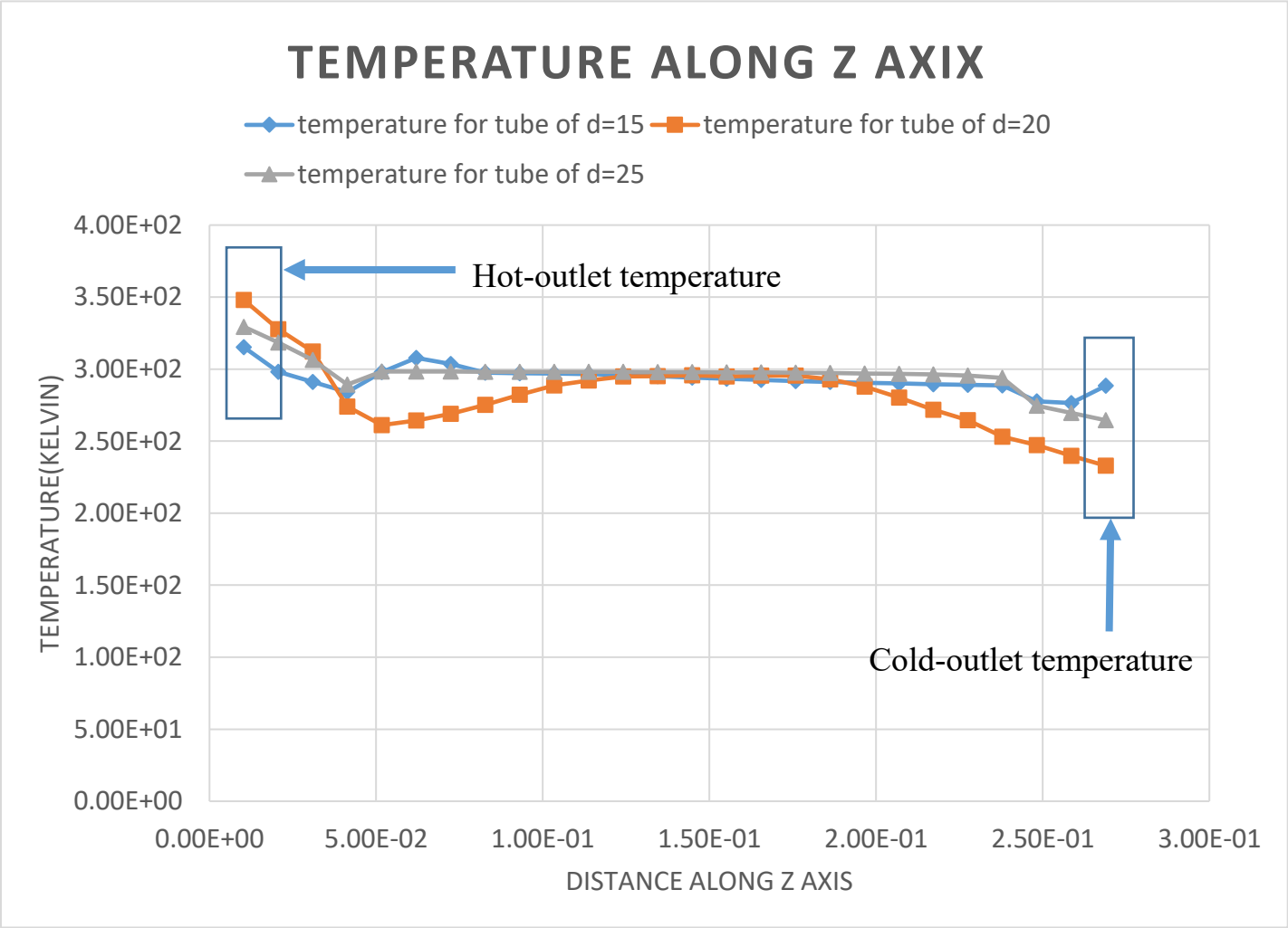

Figure 8: Comparison of temperature along the rotational axis (Z axis)

Velocity ratio refers to the ratio of the velocity of particles in a system to the maximum velocity recorded inside of that system.

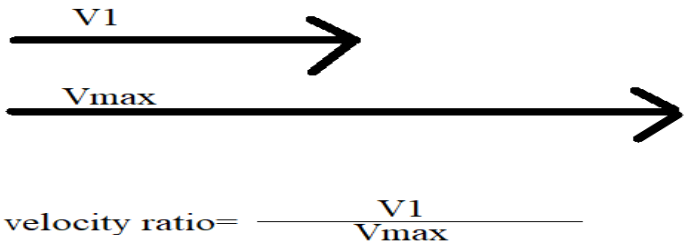

Figure 9: Velocity ratio

Two outflows of different temperature is a resultant of simultaneous transformation of energy in two different region, which are the core region and the peripheral region. Fluid particles are injected into the tube tangentially. Upon insertion they start to rotate with a larger radius of rotation in the peripheral region. Larger radius of rotation gives them greater kinetic energy which is proportional to the squared value of velocity. Greater particle velocity results in High collisional frequency of the particles. This high frequency of collision is responsible for increased temperature of the peripheral region. Velocity ratio of the particles along the axis of rotation is calculated and plotted to select the best fit geometry.

Geometry with 2 nozzles shows better performance in terms of velocity ratio. The geometry with 4 and 6 nozzles show some negative velocity ratio values at the beginning of the process as shown in Fig-7(b). This may happen due to the higher level of turbulence associated with higher number of nozzles whereas geometry with 2 nozzle shows stability throughout the tube length. So, number of nozzles for air input is selected as 2 because this geometry provides best performance in terms of velocity ratio and flow stability.

Table 4: Velocity ratio along the rotational axis (Z axis).

Z [m]	2 nozzle	4 nozzle	6 nozzle
2.69E-01	1.22E+02	-1.49E+02	-1.93E+02
2.59E-01	1.25E+02	-1.14E+02	-2.19E+02
2.48E-01	1.55E+02	-9.84E+01	-1.77E+02
2.38E-01	1.93E+02	-1.13E+02	-1.78E+02
2.28E-01	2.03E+02	-9.05E+01	-1.67E+02
2.17E-01	2.20E+02	-8.84E+01	-1.52E+02
2.07E-01	2.40E+02	-1.03E+02	-1.44E+02
1.97E-01	2.61E+02	-8.69E+01	-1.29E+02
1.86E-01	2.77E+02	-7.73E+01	-1.18E+02
1.76E-01	2.88E+02	-8.19E+01	-1.19E+02
1.66E-01	2.99E+02	-6.92E+01	-1.11E+02
1.55E-01	3.13E+02	-6.00E+01	-1.01E+02
1.45E-01	3.21E+02	-5.92E+01	-9.90E+01
1.34E-01	3.35E+02	-5.69E+01	-9.23E+01
1.24E-01	3.39E+02	-4.86E+01	-8.79E+01
1.14E-01	3.48E+02	-3.47E+01	-8.05E+01
1.03E-01	3.44E+02	-4.61E+01	-8.28E+01
9.31E-02	3.42E+02	-3.31E+01	-8.69E+01
8.28E-02	3.36E+02	-3.30E+01	-7.61E+01
7.24E-02	3.31E+02	-3.20E+01	-7.37E+01
6.21E-02	3.32E+02	-2.72E+01	-6.76E+01
5.17E-02	3.37E+02	-2.24E+01	-6.98E+01
4.14E-02	3.05E+02	-1.34E+01	-6.74E+01
3.10E-02	2.05E+02	-1.13E+01	-6.78E+01
2.07E-02	1.71E+02	-8.27E+00	-5.56E+01
1.03E-02	6.87E+01	-6.84E+00	-1.82E+01

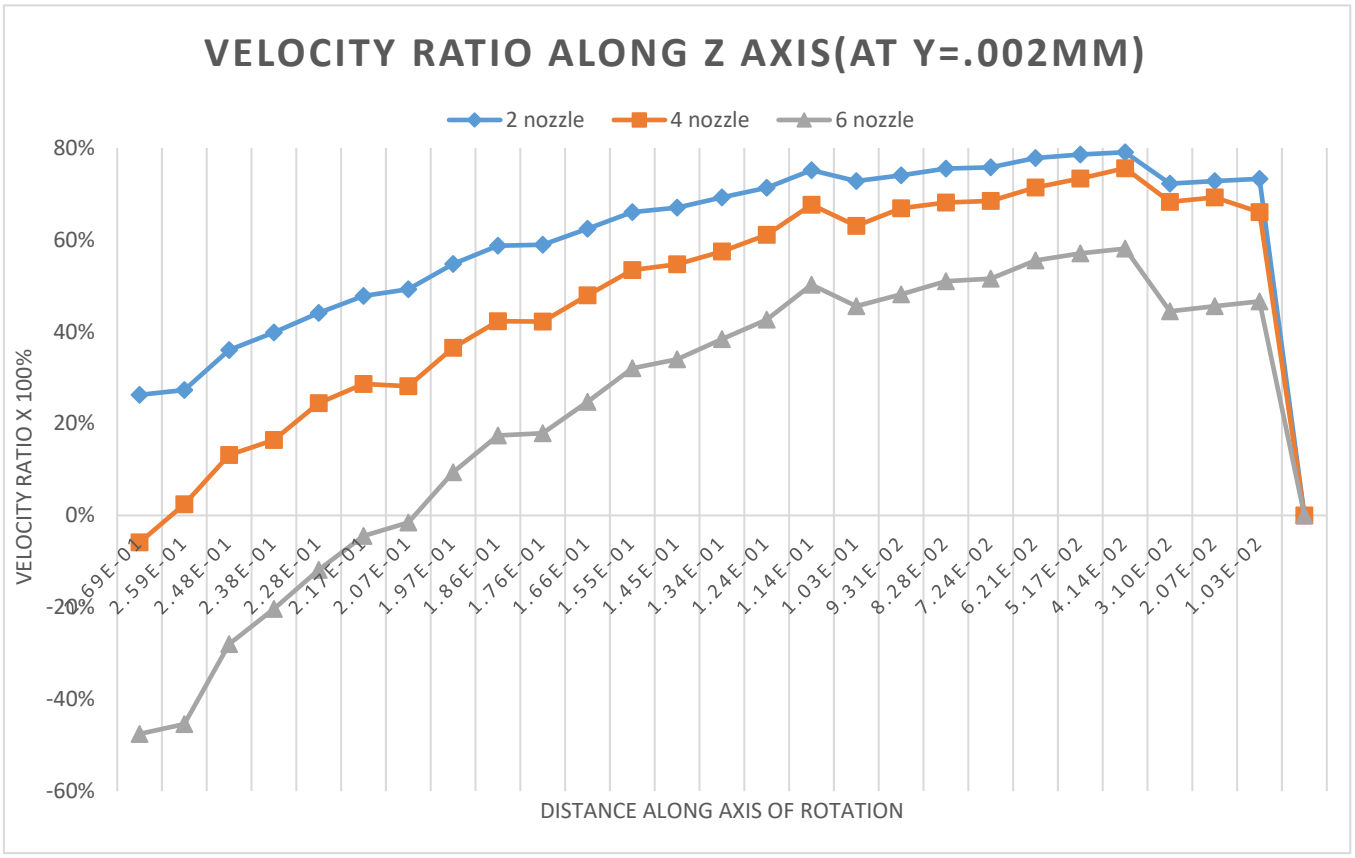

Figure 10: Velocity ratio along Z axis (at y=.002mm).

(a)

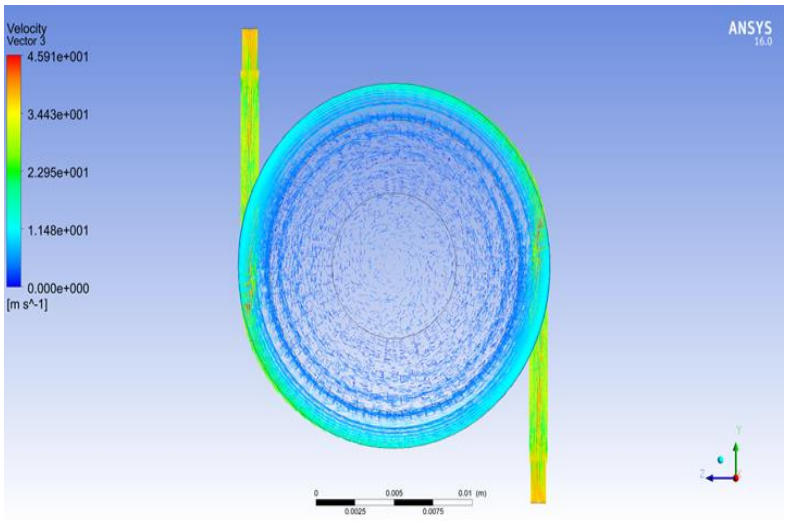

(b)

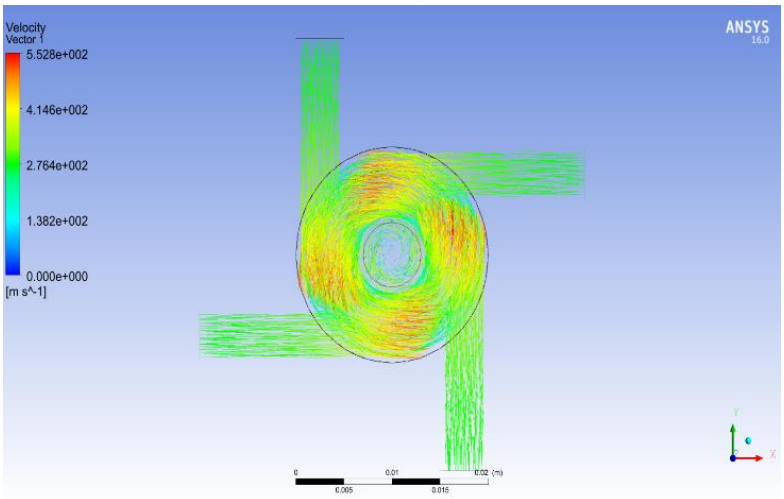

(c)

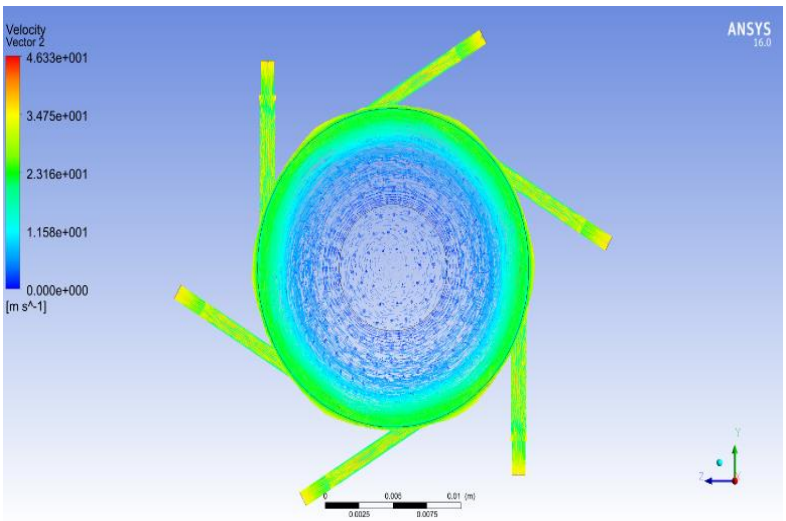

Figure 11: Swirl patterns at the inlet zone obtained from CFD for: (a) straight two numbers of nozzles; (b) straight four numbers of nozzles; (c) straight six numbers of nozzles.

Table 5: Optimized vortex-tube geometry and outlet temperatures.

Parameters	**Values**
Tube length	300 mm
Tube diameters	20mm
Inlet nozzle diameter	5mm
Cold air outlet diameter	6mm
Hot air outlet diameter	6mm
Number of nozzles	2
Hot-outlet temperature	45℃
Cold-outlet temperature	15 ℃

Chapter 4 Machining Process

4.1. Tool

To compare the three processes an identical tool is used throughout every process. The tool is selected according to recommended geometries [10] for the workpiece material (Stainless Steel) and cutting tool material (Carbide-General Insert). The geometry for the tool is given below.

Table 6: Geometric properties of the machining tool.

Parameters	**Values**
Rake Angle	-5 degree
Rake Length	2.0 mm
Relief Angle	5 degree
Relief Length	2.0 mm
Cutting Edge Radius	0.02 mm

4.2. Workpiece

As the simulation was done in a 2-Dimensional plane only the workpiece length and height were specified in the simulation software. The material chosen for workpiece is stainless steel because it's the most readily available metal. The workpiece geometry is given below.

Table 7: Geometric properties of the workpiece.

Parameters	**Values**
Height	5.0 mm
Length	30.0 mm

4.3. Process Parameters

The process parameters for the simulations are given below. They are identical for the three different processes.

Table 8: Process parameters.

Process Parameters	**Values**
Feed	0.25 mm
Cutting Speed	150 m/min
Depth of Cut	0.5 mm
Length of Cut	20.0 mm
Initial Workpiece Temperature	30.0℃
Coolant Temperature	15.0℃

Initial workpiece temperature was set to be 30 degree Celsius to simulate the effect of using vortex tube generated hot air for heating the workpiece. And the temperature at the cold outlet from ANSYS simulation was used as the coolant temperature in the AdvantEdge 3D software for the process involving vortex generated air as coolant.

4.4 Numerical Modeling

The AdvantEdge 3D software uses Finite Element Analysis (FEA) to compute various properties of the tool and workpiece at a certain time. As a machining process involves a lot of mechanical and thermo-physical phenomena, the numerical modeling of the process is difficult. So some level of generalization is established in the finite element modeling. The generalizations are listed below.

I) A 2-Dimensional simulation was carried out.

II) Chip-breakage was omitted from the simulation.

4.4.1. Finite Element Modeling

Finite element formulations are generally based on either quasi-static implicit or dynamic explicit schemes. The implicit one requires convergence at every time step or load increment and the explicit one solves an uncoupled equation system based on information from previous time steps.

Quasi-static implicit time integration schemes are largely used for metal cutting simulations. The finite element equations for Lagrangian formulations can be expressed, in general, as

$$\boldsymbol{K}_{n+1}\,\Delta\boldsymbol{u}_{n+1} = \boldsymbol{F}_{n+1} \qquad \text{and} \qquad \boldsymbol{u}_{n+1} = \boldsymbol{u}_n + \Delta\boldsymbol{u}_{n+1}$$

where $\boldsymbol{K}_{n+1}$ is the stiffness matrix, $\boldsymbol{u}_{n+1}$ is the vector of unknown incremental displacements, $\boldsymbol{F}_{n+1}$ is the load vector and $\boldsymbol{u}_{n+1}$ and $\boldsymbol{u}_n$ are the current and previous total nodal displacements. The general form of the finite element equations for Eulerian formulations can be represented as follows,

$$\boldsymbol{K}_{n+1}\,\dot{\boldsymbol{u}}_{n+1} = \boldsymbol{F}_{n+1}$$

where $\dot{\boldsymbol{u}}_{n+1}$ are the nodal velocities.

In implicit algorithms, the requirement of convergence at every solution increment provides better accuracy, however, difficulties in dealing with discontinuous chip formation and restrictive contact conditions are the main drawbacks of these schemes.

Dynamic explicit time integration schemes have been employed in metal forming problems which involve high non-linearity, complex friction-contact conditions and fragmentation. The finite element equations can be represented as

$$\boldsymbol{M}\,\ddot{\boldsymbol{u}}_n + \boldsymbol{C}\dot{\boldsymbol{u}}_n + \boldsymbol{P}(\boldsymbol{u}_n) = \boldsymbol{F}(t_n) \qquad \text{and} \qquad \boldsymbol{u}_{n+1} = \boldsymbol{u}_1 + \Delta\boldsymbol{u}_{n+1}(\Delta t, \ddot{\boldsymbol{u}}_n, \dot{\boldsymbol{u}}_n)$$

where $\ddot{u}_n$, $\dot{u}_n$ and u_{nn} are the nodal acceleration, velocity and displacement at time t_n, M and C are mass and damping matrices and P and F are internal and external forces. Although no iteration procedure is required, the stability of explicit algorithms depends strongly on the time step size, which is invariably much smaller then its implicit counterpart.

Implicit schemes can be used for simulation of continuous chip formation due to simple requirements of frictional contact. On the other hand, complex geometry and contact detection/interaction of discontinuous chip formation recommends use of explicit schemes.

4.4.2. Thermo-Mechanical Coupling

In cutting processes, energy is generated due to dissipation of both inelastic work and frictional work being transferred through the workpiece/chip and tool and lost to the surrounding environment/coolant by convection and radiation. Temperature rise causes thermal strains and affects material properties.

Thermal contact is the numerical technique to model heat transfer between chip and tool. Several approaches have been adopted, such as those presented in the following table . *Heat conduction continuity* along the chip/tool interface was used by Usui and Shirakashi (1982) which assumes an equal heat flux at the chip and tool sides of the interface [21].

Method	Equation
Heat conduction continuity	$-k_w\left(\frac{\partial T}{\partial n}\right)_w = -k_t\left(\frac{\partial T}{\partial n}\right)_t$
Constant factor	$q_w = f_c\, q_f$
Two semi-infinite bodies	$\frac{q_w}{q_t} = \frac{\alpha_t^{0.5}}{\alpha_w^{0.5}}\frac{k_w}{k_t}$ and $q_f = q + q_t$
Thermal equilibrium	$\int_w \rho_w c_w \Delta T_w dv = \int_t \rho_t c_t \Delta T_t dv$

4.4.3. Meshing Strategy

Element distortion, caused by large plastic deformation, and efforts to capture more accurately chip separation and breakage paths have been directing recent works towards the use of adaptive re-meshing procedures. The literature shows a variety of methods conceived to improve numerical solutions, such as pre-distorted meshes and local refinement. Following table shows the meshing techniques used in numerical simulations.

Technique	Observation
Pre-distorted meshes	*No re-meshing*
Local re-meshing	*Re-meshing a group of elements*
Element distortion*	*Geometrical considerations*
Rate of plastic work*	$\omega_p = \sigma_Y \dot{\varepsilon}_p$
Rate of a failure indicator*	$\dot{I}_D = \left\{ \frac{\sigma_Y^2}{2E} \left[\frac{2}{3}(1+\nu) + 3(1-2\nu)\left(\frac{\sigma_H}{\sigma_Y} \right)^2 \right] \right\}^{-s} \dot{\varepsilon}_p$

*Adaptive mesh refinement

5. Result Comparison

5.1 Stress Developed

Stress is developed in both the workpiece and tool during any machining process. Even after machining is finished residual stress remains in the tool and workpiece. This residual stress hampers the life and performance of the workpiece and it is best to keep the stress at a minimum. For comparing the stress developed during the three processes a single point on the tool and workpiece are selected for studying. The animated result for the simulation in AdvantEdge is shown for a number of time zones. The three processes are compared for a completely identical points on workpiece and tool and also identical time zones. The following tables contain the stress developed in the tool and workpiece for the three processes. All stress units are in MPa.

Table 9: Stress developed at corresponding time zones for three different processes in tool.

Zone No.	Stress Without Coolant (MPa)	Stress With Vortex Generated Coolant (MPa)	Stress With Traditional Coolant (MPa)
2	3966.02	3437.92	3806.81
5	3298.1	3647.9	3541.36
8	3689.05	3187.83	3285.8
11	3596.97	3794.93	3207.77
14	3680.33	2793.63	3143.79
17	3238.03	3371.2	3763.6
20	3799.39	2975.36	2690.21
23	4398.43	3172.23	3130.13
26	2583.63	3112.69	3725.88
29	2916.71	2763.27	2937.25
31	4419.61	3417.92	2815.43
AVG	3598.72	3243.17	3277.09

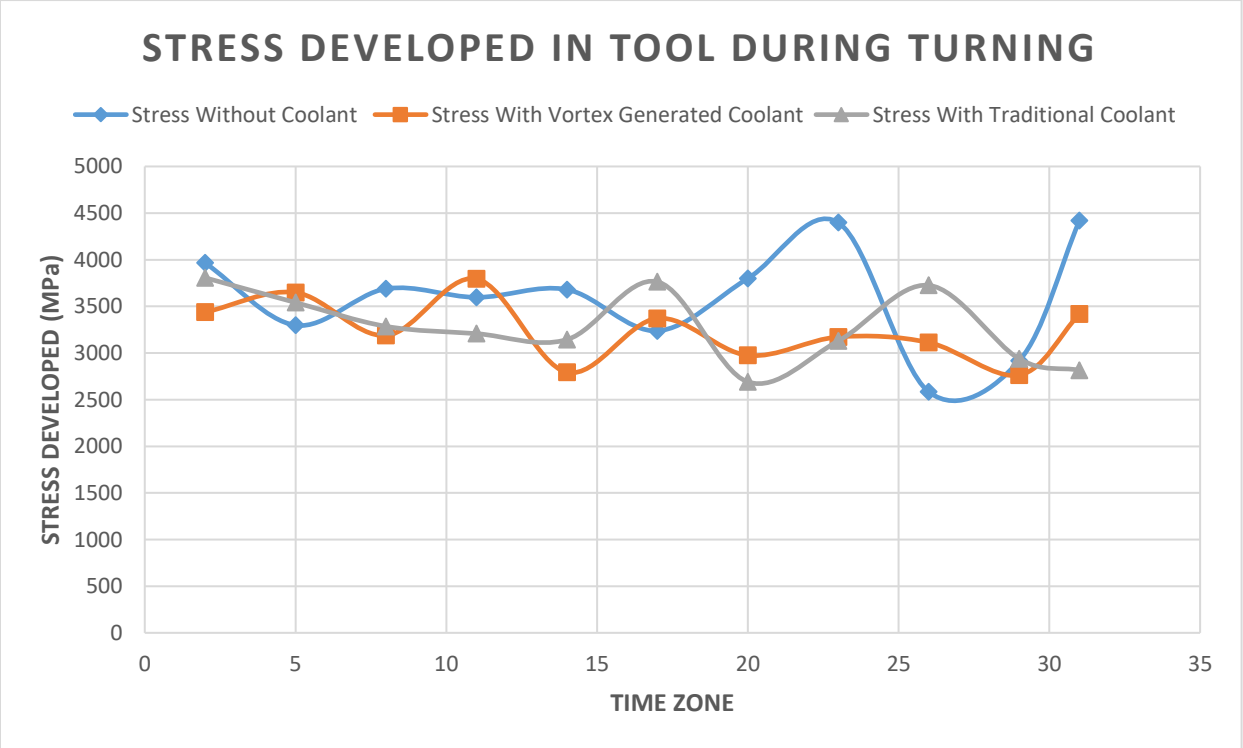

Figure 12: Stress developed at corresponding time zones for three different processes in tool.

Table 10: Stress developed at corresponding time zones for three different processes in workpiece.

Zone No.	Stress Without Coolant (MPa)	Stress With Vortex Generated Coolant (MPa)	Stress With Traditional Coolant (MPa)
2	1343.58	2859.82	1360.91
5	1684.73	2397.23	3691.55
8	2121.64	1810.23	1408.49
11	1444.5	2119.57	881.63
14	1872.02	2446.33	1601.17
17	1724.62	1663.59	2000.9
20	2144.1	1057.78	1418.27
23	933.5	1036.85	1298.36
26	1263.52	2018.14	600.32
29	1687.06	860.536	2393.9
31	2631.43	1030.45	997.99
AVG	1713.7	1754.59	1604.86

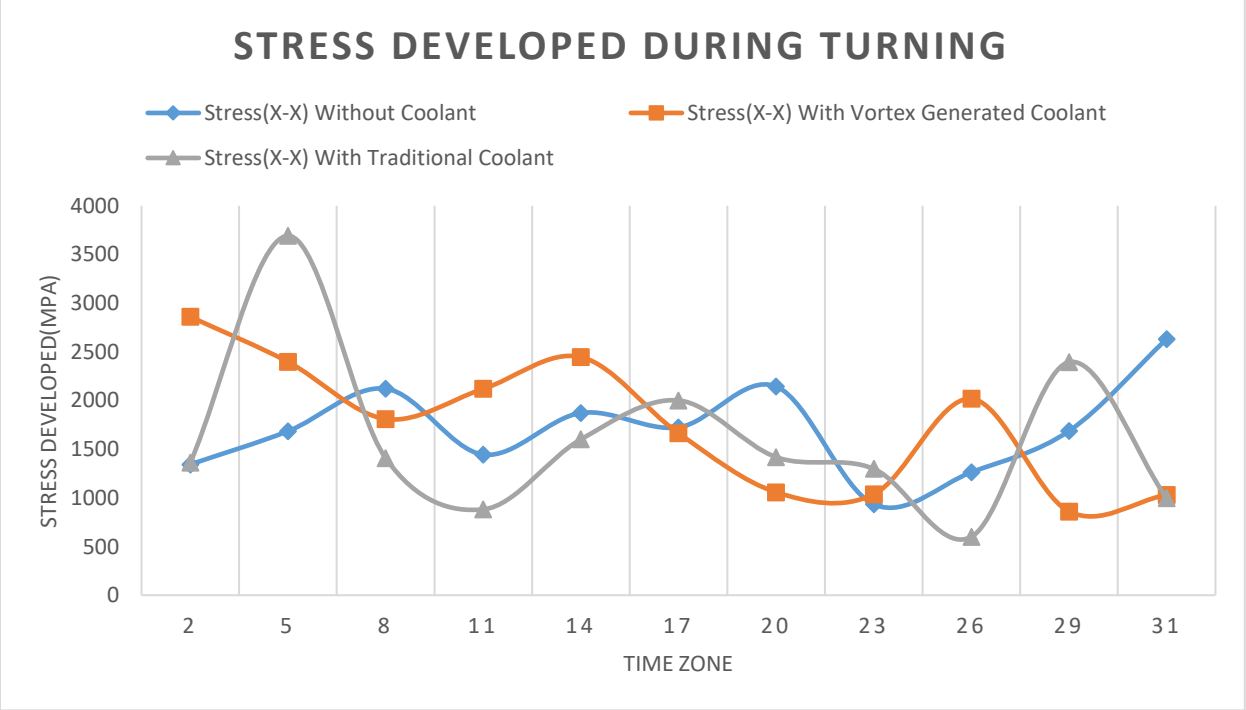

Figure 13: Stress developed at corresponding time zones for three different processes in workpiece.

As the stress varies erratically for both tool and workpiece it is difficult to compare them. So we chose to compare their average stresses.

5.1.1. For the tool (All units are in MPa)

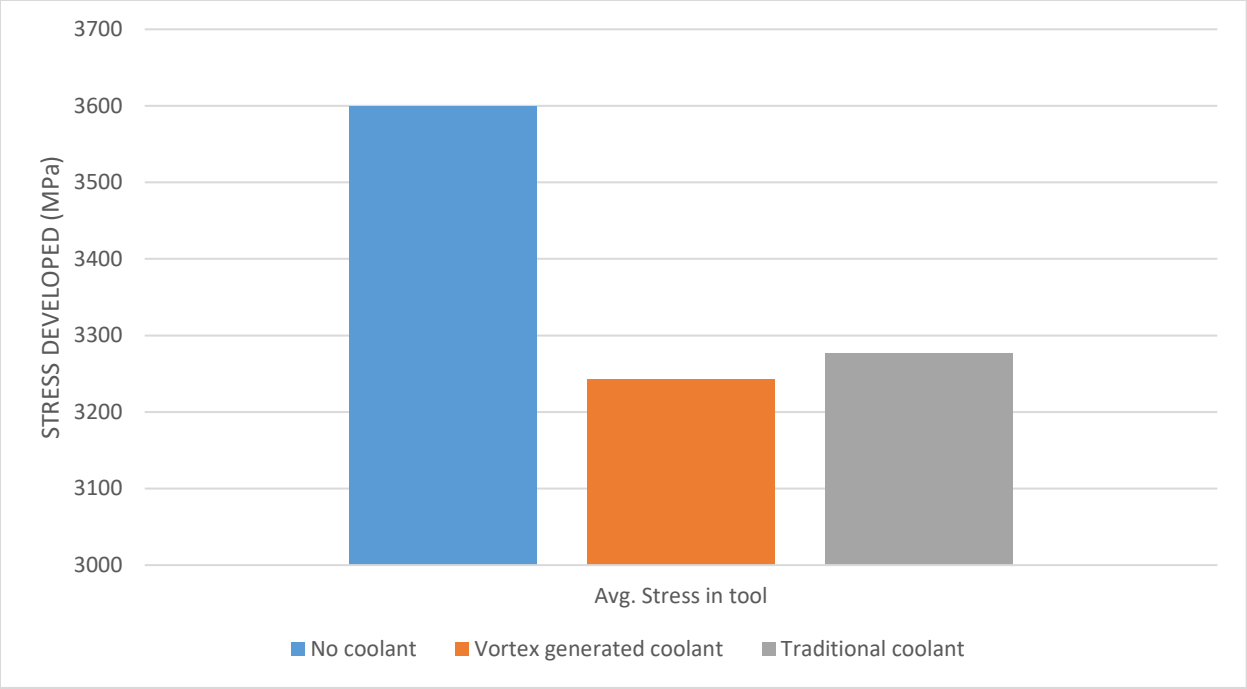

Figure 14: Comparison of average stress developed in tool.

Figure suggests that the setup with vortex generated air yields the least stress for the tool. As the stress is less the tool will undergo less wear, less deformation and the frequency of tool breakage will ultimately be reduced. Also, hot air was fed to the workpiece for the case with vortex generated coolant. This might have softened the workpiece which in turn reduced tool stress

5.1.2. For the workpiece (All units are in MPa)

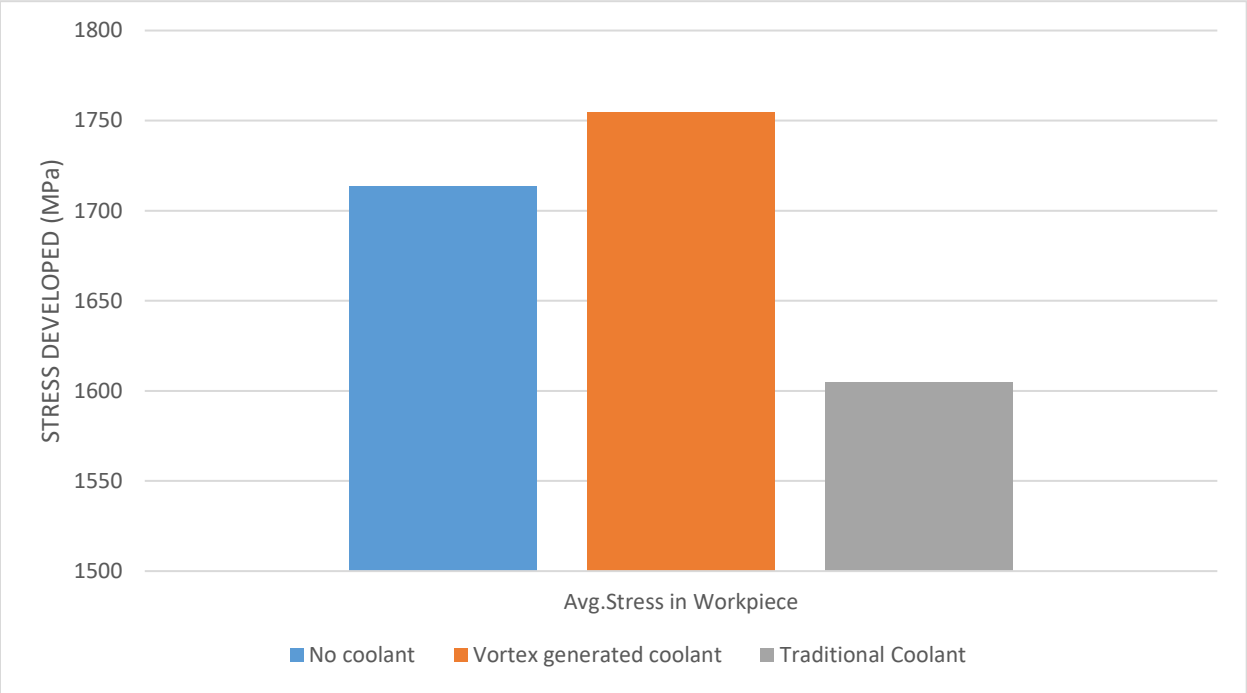

Figure 15: Comparison of average stress developed in workpiece.

The figure indicates the setup with traditional coolant yields the least stress. The probable reason behind this is that traditional coolant is liquid and vortex generated coolant is gaseous. Due to the higher viscosity traditional coolant sticks to the workpiece surface whereas gaseous coolant is in contact with the metal surface for less amount of time. So workpiece has more time to dissipate heat for traditional coolant.

5.2 Chip thickness

Chip thickness can be related to the shear plane angle and if the chip thickness is high, the shear plane angle becomes small and the chips moves away slowly on the rake face of the tool. Lower shear plane angle also requires more energy to deform the workpiece material and increases heat and cutting forces and this, in turn, increase vibration. Chip thickness was measured using a built-in tool of AdvantEdge 3D which measures distance between two points. The chip thickness measuring technique is depicted below.

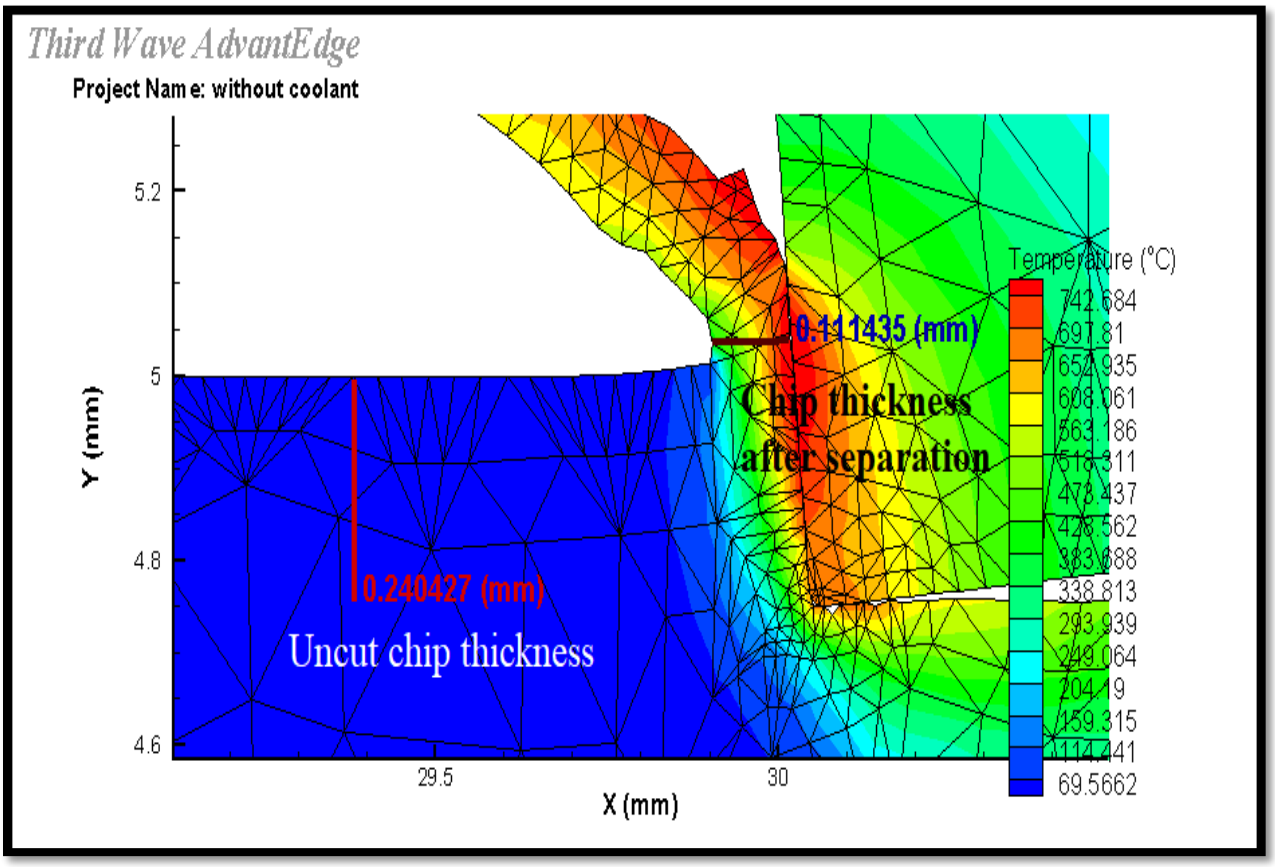

Figure 16: Chip thickness measuring technique

Chip thickness over the duration of machining varies. So for comparison purposes we will take their average chip thickness. The readings are listed below.

Table 11: Chip thickness readings.

Zone no.	Chip thickness without coolant (mm)	Chip thickness with vortex generated coolant (mm)	Chip thickness with traditional coolant (mm)
2	0.130965	0.124837	0.106017
5	0.099689	0.173007	0.134624
8	0.136829	0.127007	0.127893
11	0.115344	0.116079	0.109382
14	0.107508	0.131405	0.109434
17	0.136829	0.118248	0.127304
20	0.103617	0.11389	0.122845
23	0.115327	0.118248	0.127904
26	0.113389	0.122628	0.122845
29	0.117283	0.133577	0.114431
31	0.084052	0.124845	0.126221
Average	0.114621	0.127616	0.120809

The above readings are graphically represented below.

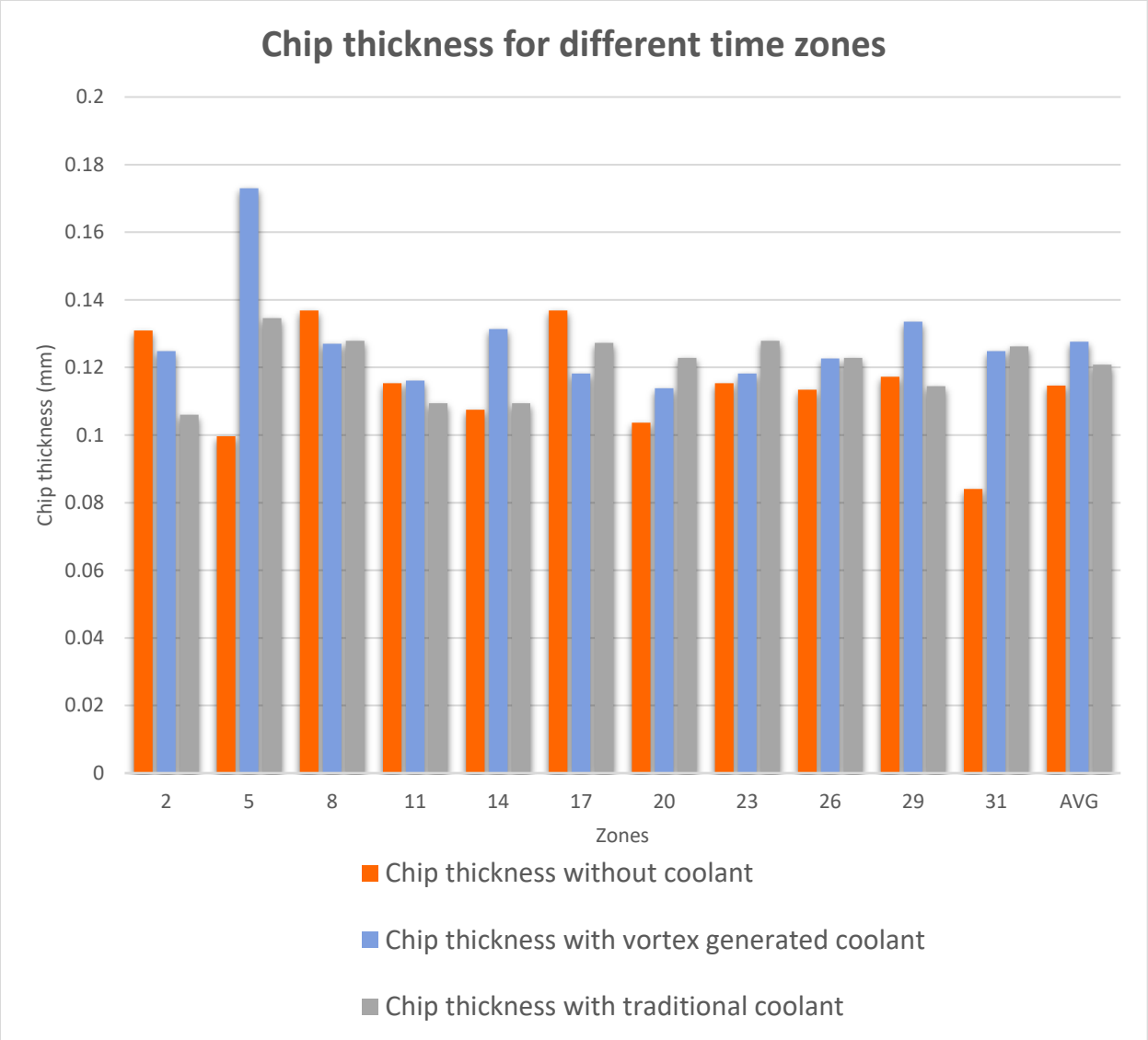

Figure 17: Comparison of chip thickness.

From the above figure we can see that vortex-tube generated coolant gives the greatest average chip thickness. So, the vortex-tube generated coolant will give us better heat dissipation, but it will also cause increased cutting force and vibration.

6. Conclusions and Recommendations

6.1. Conclusions

The purpose of this paper was to analyse the feasibility of using vortex-tube generated coolant as a replacement for traditional oil based liquid coolants. A strictly computational method was followed in this regard. Our findings can be summarised as follows :

1. **The setup with vortex generated air yields the least stress for the tool.**
   As the stress is less the tool will undergo less wear, less deformation and the frequency of tool breakage will ultimately be reduced. Hot air was fed to the workpiece for the case with vortex generated coolant. This might have softened the workpiece which in turn reduced tool stress.

2. **The setup with traditional coolant yields the least stress.**
   The probable reason behind this is that traditional coolant is liquid and vortex generated coolant is gaseous. Due to the higher viscosity traditional coolant sticks to the workpiece surface whereas gaseous coolant is in contact with the metal surface for less amount of time. So workpiece has more time to dissipate heat for traditional coolant.

3. **The readings for the chip thickness are almost identical for all three cases.**
   This was expected because the depth of cut was kept constant (0.5mm). By inspecting the average chip thickness we see that vortex-generated coolant gives greater chip thickness compared to the other two cases. Greater chip thickness means greater surface area which in turn increases heat dissipation. Studies [22] have also revealed that greater chip thickness means lower shear plane angle. Increased power is required to deform the workpiece for lower shear plane angle. Increased power means cutting force and vibration during machining will be higher.

6.2. Recommendations

- As this paper includes only numerical approach, further research using a physical setup might reinforce the feasibility of cold air as replacement of liquid coolant.
- In future , effects of other gasses like CO_2, N_2, He, H_2, CH_4 et cetera can be evaluated as coolant in the machining process.

Chapter 7 Bibliography

[1] R. G. J., "Experiments on whirling and simultaneous production of an exhaust air outlet and a cold air exhaust".

[2] R. Hilsch, "The Use of the Expansion of Gases in a Centrifugal Field as Cooling Process".

[3] S. L. M. D. H. D. S. K. Stephan, "An investigation of energy separation in a vortex tube".

[4] R. Liepmann, "A 17-Inch Diameter Shock Tube for Studies in Rarefied Gasdynamics".

[5] P. Deissler, "Analysis of the flow and energy separation in a turbulent vortex".

[6] L. Linderstorm, "Gas separation in the Ranque-Hilsch vortex tube".

[7] E. E. J.P. Hartnett, "Experimental study of the velocity and".

[8] J. J. Keyes and R. Dial, "AN EXPERIMENTAL STUDY OF VORTEX FLOW FOR APPLICATION TO GAS-PHASE FISSION HEATING".

[9] Lay, "An experimental and analytical study of vortex flow temperature separation by superposition of spiral and axial flows".

[10] A.J.Reynolds, "A note on vortex-tube flows".

[11] R. Savino, "Some Temperature and Pressure Measurements in Confined Vortex Fields".

[12] B. Scheller, "The Ranque-Hilsch Vortex Tube".

[13] B. S. Takahama, "Studies on Vortex Tubes : (1) Experiments on Efficiency of Energy Separation : (2) On Profiles of Velocity and Temperature".

[14] B. Syred, "A review of oscillation mechanisms and the role of the precessing vortex core (PVC) in swirl combustion systems".

[15] A. e. al, "Cutting Tool Materials and Tool Wear".

[16] H.R.Thakre, "CFD analysis of energy separation of vortex tube employing different".

[17] David.A.Field, "Qualitative measures for initial meshes".

[18] Z. Y. Jun Wang, "Quality mesh smoothing via local surface fitting and optimum projection".

[19] C. K. L. G. V. E. Y. K. Lee, "Surface mesh generation for dirty geometries by the Cartesian shrink-wrapping technique".

[20] U. b. e. al, "CFD analysis and experimental investigations towards".

[21] S. Usui, "Analytical Presumption of Cutting Tool Wear in Machining with Chatter Vibration".

[22] I. K. e. al, "Determination of optimum cutting parameters during machining of austenitic stainless steel".

[23] "(Hashemi et al., 1994; Marusich and Ortiz, 1995; Vaz Jr. et al., 1998a; Vaz Jr. et al., 1998b; Owen and Vaz Jr., 1999).," [Online].